[Frontiers in Bioscience E2, 339-350, January 1, 2010]

Multilayer CuHCF films bridged by CuMPCs for H_2O_2 detection

Qin Xu[1,2], Bo Liu[1], Xiao-Ya Hu[2], Jun-Jie Zhu[1]

[1]Key Lab of Analytical Chemistry for Life Science(MOE), School of Chemical and Chemistry Engineering, Nanjing University, Nanjing, 210093, P. R. China, [2]College of Chemistry and Chemical Engineering, Yangzhou University, Yangzhou, 225002, P. R. China

TABLE OF CONTENTS

1. ABSTRACT

Multilayer copper hexacyanoferrate (CuHCF) films bridged by cysteine monolayer protected copper clusters (CuMPCs) were prepared by the sequential electrochemical cyclcing and dipping process. Cyclic voltammetry, scanning electron microscopy (SEM) and atomic force microscopy (AFM) were used to characterize the formation of the multilayer films. Cyclic voltammetric measurements indicated that the films grew exponentially with the increase of the layer numbers. AFM and SEM images revealed that the obtained films were thin and exhibited a three-dimensional structure. The nanostructured thin-film assemblies exhibited interesting catalytic properties that could be applied in important sensing and catalysis. Good catalytic activity and stability of the film modified electrode for hydrogen peroxide detection was studied.

2. INTRODUCTION

Hydrogen Peroxide (H_2O_2) is a side product of oxidases which is included in more than 90% of the existing enzyme-based biosensors and analytical kits (1). It is also recognized as one of the major risk factors in progression of disease-related pathophysiological complications in diabetes, atherosclerosis, renal disease, cancer, aging, and other conditions (2). Monitoring of low levels concentration of H_2O_2 at low-potential is of practical importance in food, pharmaceutical, chemical, biochemical, industrial and environmental analyses (3). Recently metal hexacyanoferrates have been widely used as H_2O_2 transducers because of their high activity and selectivity (4-5). Among different analogues, copper hexacyanoferrates have received special attention (6). However, to the best of our knowledge, there are no reports on the preparation of the three-dimensional multilayer CuHCF films and their application as the H_2O_2 biosensor.

Multilayer films showed some advantages as sensing and electronic devices because of their thickness controllability and composite adjustability (7). The loading density of the particles on the films would improve their application performance in sensitivity (8). Examples included DNA complimentary binding (9-11), polymer or dendrimer mediated assemblies (12-15).

The compounds with carboxylate groups have excellent recognition properties for metal ions (16-17), and the studies in the formation of multilayer films based on the molecules with straight alkyl chains have been undertaken (18-19). However, these films have some disadvantages such as strictly two-dimensional surfaces and limited stability (20-21). These shortcomings could be overcome by enhancing the functional group density and increasing the dimensionality of the films.

Nanometer-sized particles with functional groups have been the subject of increasing attention for the past decade due to their potential applications in catalyst, heavy-metal detection and chemical sensing (22-23). A facile synthesis of nanoparticles composed of gold clusters coated with thiolate monolayers (Au MPCs), introduced by Schiffrin and his co-workers, has attracted extensive use (24). The obtained MPCs exhibit stability in both solution and dry forms. It is most important that a wide variety of structural groups could be introduced into the nanoparticles (25-28). It indicated the feasibility of forming different kinds of multilayers based on them. The quasi-three-dimensional surfaces yielded by MPCs would provide higher functional group density than the linear, alkyl-based self-assembled multilayers (SAMs). The stability of the obtained film could also be increased by the multipoint binding character of MPCs.

Herein, we synthesized the cysteine encapsulated copper nanoparticles (CuMPCs) by using one-phase method. Cysteine, as a kind of water soluble amino acid, has three main functional groups (Figure 1), the amino and carboxylate functionalities, and the terminal thiol group. The adsorption of cysteine on different metal surfaces such as gold and copper has been reported (29-30). Because multilayer films based on the interaction of copper ions with carboxylic acid group were reported (31), we reasoned that a similar chemistry could be envisaged to fabricate multilayer films based on the cysteine protected copper clusters. The fabricating process was shown in Figure 1. CuMPCs were anchored on the electrode by potential cycling, and then, the CuMPCs modified electrode was dipped into potassium ferricyanide solution to form CuHCF nanoparticle overlayer by ionic interactions. Multilayer CuHCF films could be formed by the repetition of the sequential processes. The films were characterized by cyclic voltmmetry, atomic forced microscope (AFM) and scanning electron microscopy (SEM), respectively, and were used as the hydrogen peroxide sensor.

3. EXPERIMENT SECTION

3.1. Chemicals

$CuSO_4 \cdot 5H_2O$, L-Cysteine hydrocloride, KBH_4 and potassium ferricyanide were obtained from Shanghai Chemical Reagent Factory and used as received. All other reagents were of analytical grade and used without further purification. Pure water was obtained by Millipore Milli-Q water purification system (Millipore Co. Ltd., USA), and the resistivity was18.6MΩ.

3.2. Instruments

Electrochemical experiments were carried out on CH Instrument (Shanghai ChenHua, China) Model 630 electrochemical workstation. All electrochemical measurements were performed in a three-electrode electrochemical cell with a saturated calomel reference electrode (SCE), a platinum foil counter electrode, and an indium tin oxide (ITO) or a glassy carbon working electrode (d = 3 mm). Indium-doped tin oxide (ITO) glasses were purchased from Zhejiang Jinhua Baolai Vacuum Filming Co., Ltd (Zhejiang, China). They were previously sonicated in acetone for 5 min, followed by rinsing with water and drying before the experiments. The glassy carbon electrode was firstly polished with 0.015 μm aluminum slurry (BDH Chemicals Ltd Poole England), then sonicated successively in redistilled water and ethanol, and finally rinsed thoroughly with redistilled water. The Fourier Transform Infrared (FTIR) spectra of cysteine and CuMPCs were measured using a Nocolet 400 Fourier transform infrared spectrophotometer (Nocolet, USA). Transmission electron image (TEM) was recorded on a Hitachi 8100 transmission electron microscope, using an accelerating voltage of 200 keV. SEM images were taken on a LEO-1530VP field-emission scanning electron microscope. AFM measurements were performed with SPI-3800N (Seiko, Japan) atomic force microscopy. "Tapping mode" measurements were used to avoid the damage of the films. Multiple images at different areas of each film were taken.

3.3. Preparation of CuMPCs

The synthesis of the CuMPCs with cysteine as the capping molecules was as follows: 5 ml of 0.01M L-cysteine hydrochloride was added into 5 ml of 0.01M $CuSO_4 \cdot 5H_2O$ aqueous solution while the solution was stirred violently. It was found that the solution became gray and then 0.080g of KBH_4 dissolved in 5ml ice water was added slowly. The solution quickly turned into ruby-red, indicating the formation of the copper particles. After the solution was continuously stirred for 3 hours, the CuMPCs were obtained. CuMPCs were purified from free cysteine molecules using the standard precipitation-redispersion protocol. Typically, the as-synthesized particle solution was mixed with an equal volume of methanol to precipitate the particle. Then the solid was suspended in a 1:4 mixture of water and methanol, and was isolated by repeated ultracentrifugation.

3.4. Preparation of multilayer CuHCF films

The process for the fabrication of multilayer CuHCF films included two steps: (1) cycling the electrode

between the potential of –0.8 and 0.6 V in CuMPCs

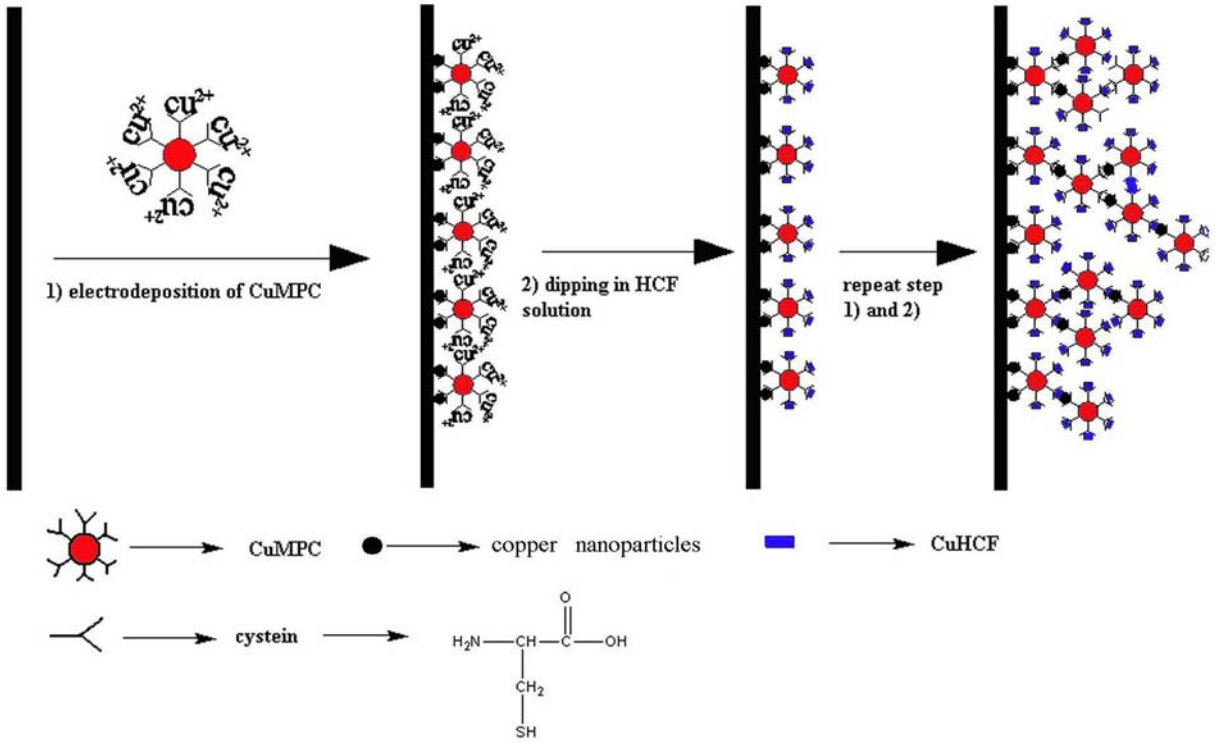

Figure 1. The fabrication process of the multilayer CuHCF.

solution at a scan rate of 50 mVs^{-1} for 20 cycles to anchor CuMPCs onto the electrode; (2) dipping the obtained electrode into 10 mM potassium ferricyanide aqueous solution at ambient temperature for 20 min, which resulted in the formation of the first layer CuHCF film surrounding CuMPCs. Repetition of the two steps would lead to the formation of multilayer CuHCF films that bridged by CuMPCs. The CuMPCs solution used was prepared as follows. All the obtained CuMPCs was dispersed in 10 mL water and then the pH of the solution was adjusted to about 9.0 using NaOH. The experiments were all performed at room temperature.

4. RESULTS AND DISSCUSSION

4.1. Characterization of CuMPCs

TEM observation was used to determine the size and morphology of CuMPCs, and the image is shown in Figure 2. The nanoparticles was found to be nearly monodisperse, and their size distribution is about 5-10 nm. The resulting nanoparticles could be used as the starting materials for the multilayer formation procedures.

The FTIR spectra of pure cysteine and CuMPCs taken in a KBr pellet were collected over the range of 400–4000 cm^{-1} in the transmission mode. As shown in Figure 3, the spectrum of CuMPCs was similar to that of pure cysteine molecules. The 3100 cm^{-1} band is attributed to the asymmetric and symmetric C-H stretching and 1620 cm^{-1} signal is assigned to the C=O stretching. The 1100cm^{-1} signal is attributed to C-O stretching vibrations. All those bands were observed in both cysteine and CuMPCs samples. The N–H stretch of cysteine molecule was observed at 3343 cm^{-1} (Figure 3 a), and that of CuMPCs functionalized with cysteine was observed at 3342 cm^{-1} (Figure 3 b). The peak positions of them are almost the same. It suggested that the $–NH_2$ group didn't interact with copper particles. However the small peak at 2550 cm^{-1}, corresponding to the S–H stretching vibration mode, disappeared when the cysteine molecules adsorbed on the Cu nanoparticle surface (Figure 3 b), giving strong evidence that cystein anchored on the copper surface through the sulfur atom in the mercapto group (32). All those evidences agreed well earlier studies on cysteine modified silver nanoparticles (33).The carboxylate ligand (1620 cm^{-1}) of cysteine could form a salt with copper ions (18) and the salt was thought to be responsible for the formation of CuHCF nanoparticles (34).

Potentiodynamic technique could be used to directly deposit CuMPCs on the electrode surface. It has been reported that the effectiveness in preventing surface oxidation of copper nanoparticles was poor. High air sensitivity of copper nanoparticles needs extremely careful and challenging approaches to avoid the oxidation of copper nanoparticles. Oxygen can penetrate the surface of the copper nanoparticles especially in aqueous medium, and make them oxidized. In our experiment, the copper nanoparticles were oxidized slowly with O_2 as the electron acceptor (35). So there is free Cu^{2+} presented although excess amount of KBH_4 has been used. During the electrochemical deposition process, some of these copper ions could be deposited on the electrode. Through the

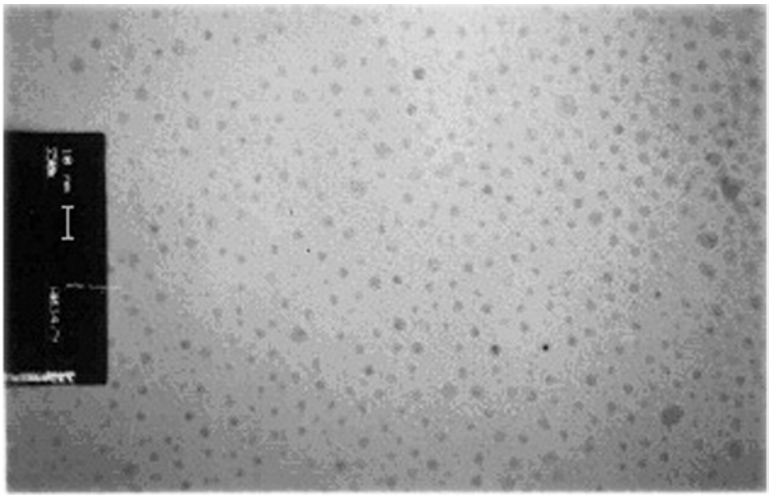

Figure 2. TEM image of the CuMPCs. The scale bar of the image is 10 nm

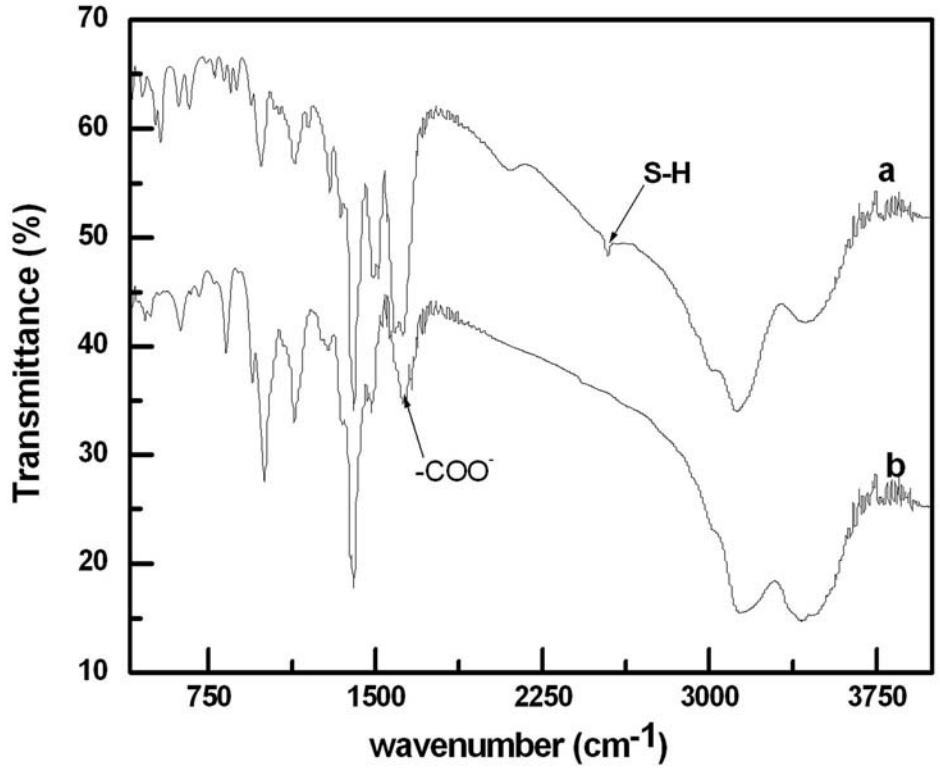

Figure 3. FTIR spectra of (a) cysteine and (b) CuMPCs.

interaction between cysteine and the electrodepositied copper nanoparticles, CuMPCs have been modified on the electrode. The typical current-potential characteristic of the CuMPCs deposition process in the potential range of –0.8 to 0.6 V is shown in Figure 4. The anodic waves labeled I_o, II_o correspond to the formation of Cu(I) and Cu(II) while the cathodic peaks marked II_R, I_R represent the reduction of Cu(II) to Cu(I) and Cu(I) to Cu(0). After 20 scan cycles were carried out, the electrochemical process became reversible. The charges associated with the stripping process and redeposition process were almost the same, indicating that the deposited CuMPCs became constant (36).

4.2. Formation of multilayer CuHCF films bridged by CuMPCs

Figure 5 A shows the voltammetric characteristic of the first layer CuHCF film modified electrode in 0.1 M KCl solution. The first monolayer CuHCF shows three oxidation peaks. The peak at 0.38 V (I_o) corresponds to the oxidation of Cu(0) to Cu(II), which is reduced at 0.04 V (I_R) (37). The second peak at 0.50 V is attributed to the

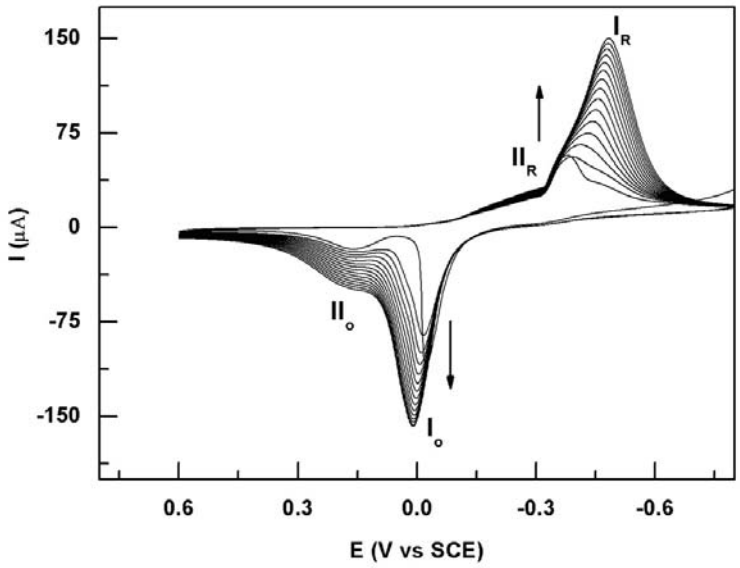

Figure 4. Electrodeposition of CuMPCs on the glassy carbon electrode. The scan rate is 50 mv/s.

oxidation of a Cu(I)-thiolate species (38). The pair of quasi-reversible peaks at about 0.70 V can be described as follows:

$$KCu[Fe^{3+}(CN)_6]+K^+ +e^- \rightarrow K_2Cu[Fe^{2+}(CN)_6]$$

These peaks were assigned to the low-spin FeII/III redox couple in the CuHCF, which was similar to the transition metals reported by Kuwana for CuHCF (37), and the peaks were used to characterize the growth process of the multilayer films. In contrast, when $CuSO_4$ solution in pH 9.0 solution was used as linkers instead of CuMPCs, no peak was observed (Figure 5 B), which indicated that CuMPCs played an important role in the formation of CuHCF films. Cysteine is an interesting amino acid that contains three dissociable protons (pK_{COOH} =1.91, pK_{NH3}= 8.16 and pK_{SH} = 10.25). The thiol group in cysteine was capable of chemisorbing on copper surface in the preparation of CuMPCs. So it formed a monolayer on the copper nuclei surface with the carboxylic acid and amino groups pointing outward (33). In the basic deposition solution, this monolayer around copper cores became deprotonated, and a carboxylate/Cu(II) complex was formed. The metal salt formed in the copper ions and the carboxylic acid on the CuMPCs surface could react with ferricyanide to form CuHCF nanoparticles.

The electrochemical response of CuHCF at 0.7 V increased when CuMPCs was used as the linkers, indicating the increase of CuHCF density. A series cyclic voltammograms with different layers are shown in Figure 6. The inset of Figure 6 depicted the charge under the redox peak at 0.70 V as a function of number of layers of CuHCF film. Rather than a linear growth profile, which is typical for most electrostatic layer-by-layer assembled films (39), the films linked by CuMPCs first evolves exponentially with the number of deposition steps. After a given number, it follows a linear evolution. The exponential growth is always associated with the increase of surface roughness (40) and "heterogeneous" film topography (41). CuMPCs was a kind of nanoparticles with roughness surface, so it could present an increasing surface area, which increased the amount of the deposited CuHCF nanoparticles. On the other hand, the hexacyanoferrate ions could move into the bottom of the layer during each layer pair deposition step, and caused the heterogeneous topography (42). Therefore the exponential growth came from the increase of the film roughness and the "heterogeneous" film topography in the buildup process.

In all MHCF inorganic compounds, the Fe(III)/Fe(II) unit can undergo one electron reversible oxidation process. The ninth layer of the CuHCF film grown on the glassy carbon electrode has been examined by cyclic voltammetry in KCl aqueous solutions, as shown in Figure 7. The separation between the anodic and cathodic peak potential of Fe(II) to Fe(III) occurring at 0.70 V was quite small. It indicated that the species were surface bound and the electron transfer was facile. The peak currents showed a linear dependence with square root of the scan rates, which suggested thin films were formed, and the electrochemical reaction of Fe(III)/Fe(II) unit in the multilayer assemblies was a diffusion-controlled redox process (43-44).

Immobilization of CuMPCs and CuHCF on the electrode was characterized by SEM to assess the layer surface topography. Typical SEM images of the CuMPCs and the ninth layer films are showed in Figure 8. Figure 8 A showed a homogenous globular dispersion of CuMPCs which were distributed separately on the surface of ITO electrode. A vermiculate pattern was observed in the ninth layer CuHCF film as shown in Figure 8 B and Figure 8 C, which was similar to those observed by McAloney (45). The vermiculate surface pattern was associated with the

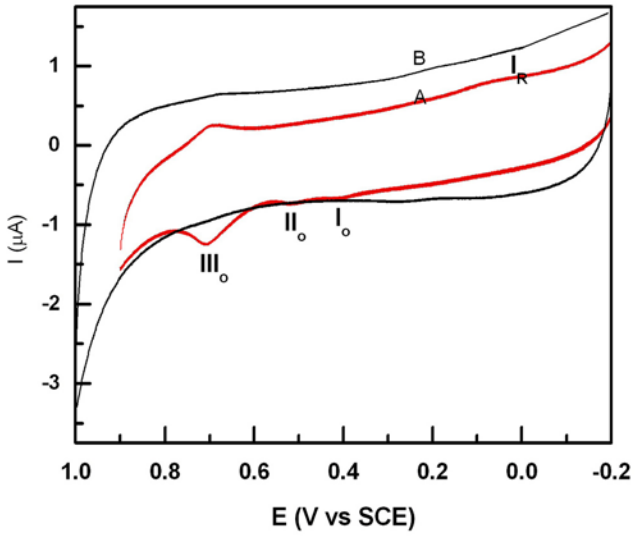

Figure 5. Cyclic voltammograms of the first layer CuHCF using MPCs (A) (red line) and $CuSO_4$ (B) (black line) as the precursor.

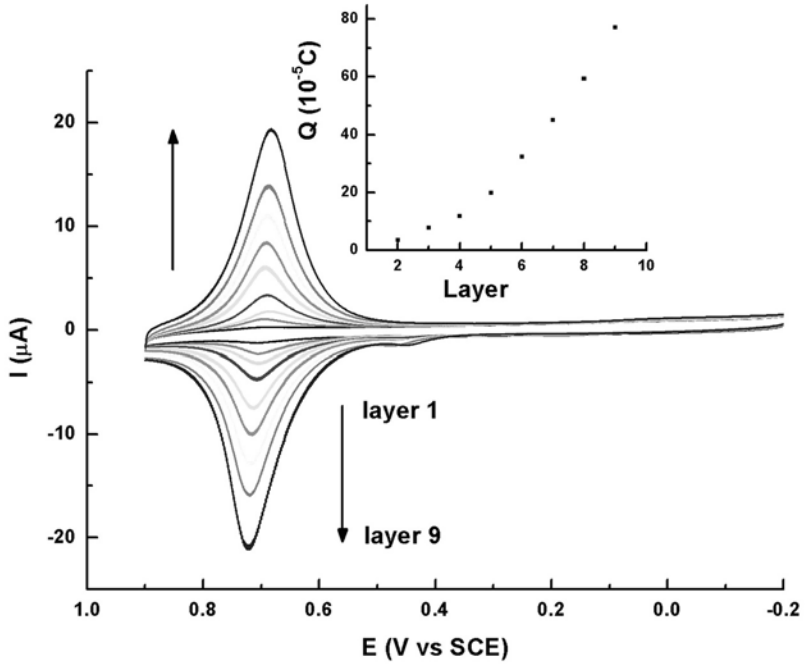

Figure 6. Cyclic voltammograms of the 1-9 layers CuHCF film in 0.1 M KCl solution at a scan rate of 100 mV/s. Inset was the Faradic charge associated with low-spin $Fe^{2+/3+}$ redox center as a function of number of layers of CuHCF.

increase of the film roughness (46), which might be attributed to the particular effect of CuMPCs. The multilayer CuHCF films were bridged by CuMPCs and formed three-dimensional networks. The network could increase the surface area of the films.

To clearly investigate the film growth processes, a series AFM images are presented in Figure 9. For a comparison, an AFM image of the bare ITO electrode was shown in Figure 8 a. It was flat and only little bright dots were distributed over it. These bright dots were the defect of ITO electrode itself. In contrast, an evident change in morphology was observed after the deposition of the CuMPCs layer. Figure 9 b presents the topographic images of the first layer CuMPCs modified electrode by potential cycling in CuMPCs solution for a fixed 20 cycles. The smaller and spherical nanoparticles distributed over the electrode surface were observed, which demonstrated that

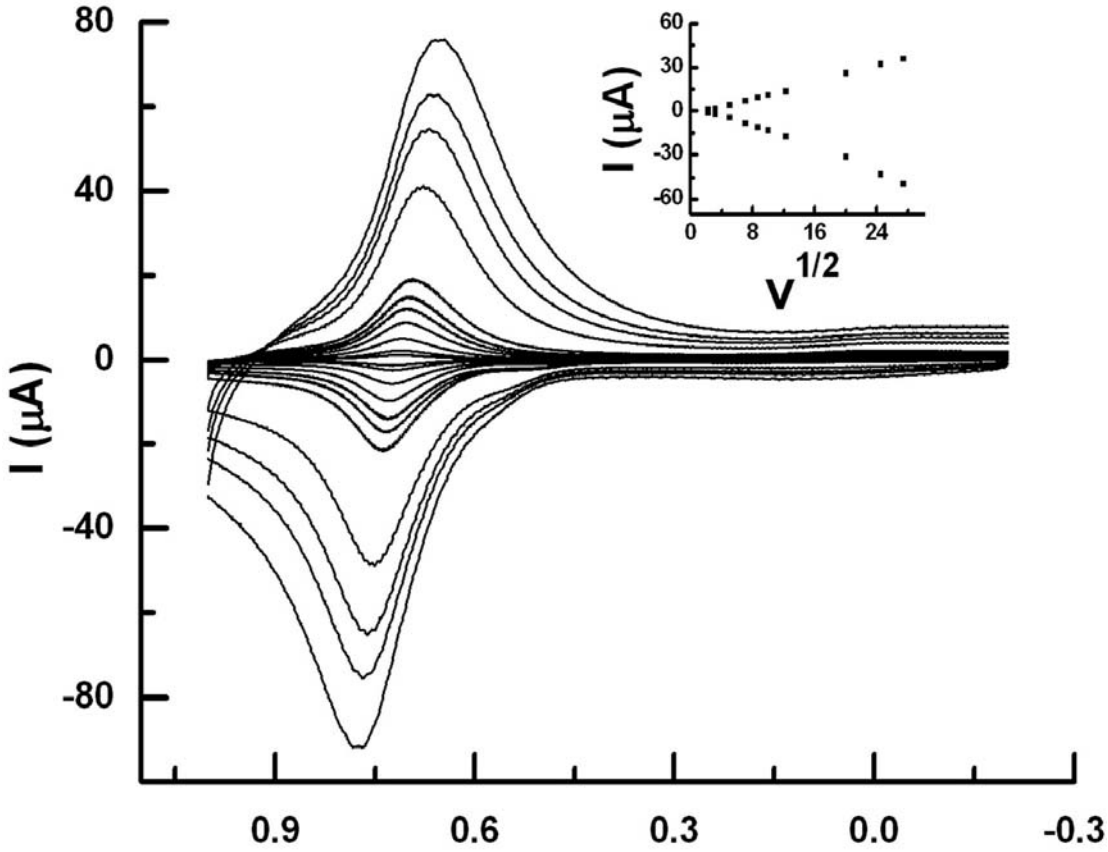

Figure 7. Cyclic voltammograms of the ninth layer CuHCF modified electrode in 0.1 M KCl solution at various scan rates. Inset was the relationships of the oxidation and reduction peak currents vs the square roots of the scan rate.

CuMPCs was successfully anchored on the electrode. Significant difference was also observed when the electrode was exposed to the ferrocyanide solution for 20 min. Figure 9 c shows the 3 layer film for the CuHCF. The surface of the multilayer CuHCF was composed of nanoparticles with average diameter of 6-10 nm. These particles were dispersed uniformly on the surface. Each granule showed the increase in assembly thickness with the increase of the layer number. Therefore, CuHCF films have been successfully formed and anchored on the electrode by the electrochemical/chemical process. The number of dots per unit area increased slightly with the building up of the multilayers. Figure 9 d showed the topography of the ninth layer of CuHCF modified ITO electrode. In the image, a dense film was formed. When the electrode was cycled in $CuSO_4$ solution, the topographic images was almost flat (Figure 8 e), which indicated that the globular nanoparticles were CuMPCs.

The proposed mechanism for the controlled growth of the multilayer CuHCF films bridged by CuMPCs was discussed. One possible reason is the attachment of $-NH_2$ of cysteine on the Cu sites located on the CuHCF surface (47). In a contrast experiment, the electrode modified with one layer CuHCF film was dipped into the CuMPCs solution for 20 min without applying potential, and then the electrode was taken out to dip into ferrocyanide solution for another 20 min. It could also observe that the signal of CuHCF at 0.7 V increased slightly. It suggested multilayer CuHCF films could be formed by the layer-by-layer method. However the slightly increase of the signal indicated the low assembling efficiency of the CuHCF in the absence of electric field. When electrochemical method was used, the signal increased greatly. The as-prepared CuHCF nanoparticles may act as the nucleation centers and catalyze the formation of the next layer CuHCF. The other possible explanation came from the substantial different activation barriers for the ion transfer reactions (48). According to the classic theory of nucleation and growth (49), the free energy to form stable nucleation on a substrate is determined by the following equation:

$$\Delta G = -RT \ln S + \sigma_{cl} + (\sigma_{cs} - \sigma_{sl}) A_{cs}$$

Where S is the degree of supersaturation, σ_{cl} is the interfacial energy between the particle (c) and the liquid (l), σ_{cs} is the interfacial energy between the particle and the substrate (s), σ_{sl} is the interfacial energy between the substrate and the liquid, and A is the surface area of the particle. In the CuMPC solution, only part of the Cu-S bond was breakdown, so the copper ions concentration was low, which would control the copper nucleus on the electrode.

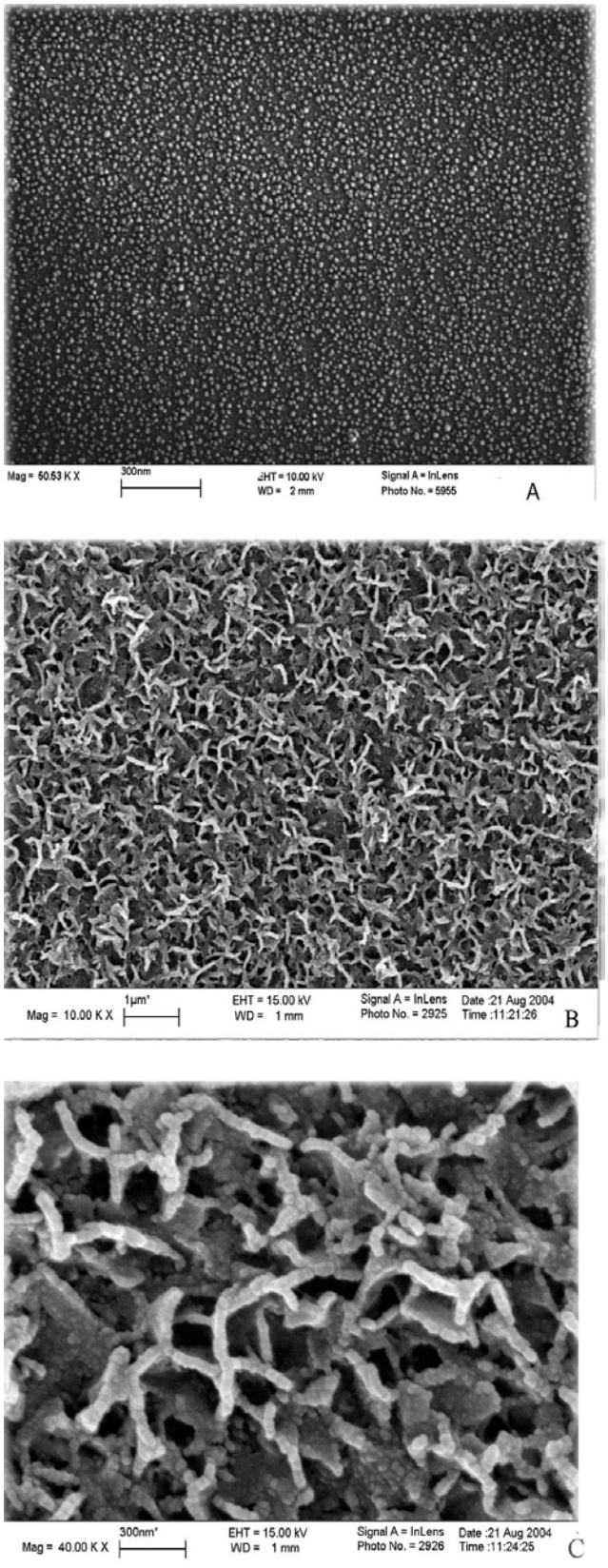

Figure 8. SEM images of the CuMPCs modified ITO electrode (A) and the ninth layer CuHCF (B). C is the enlargement of B.

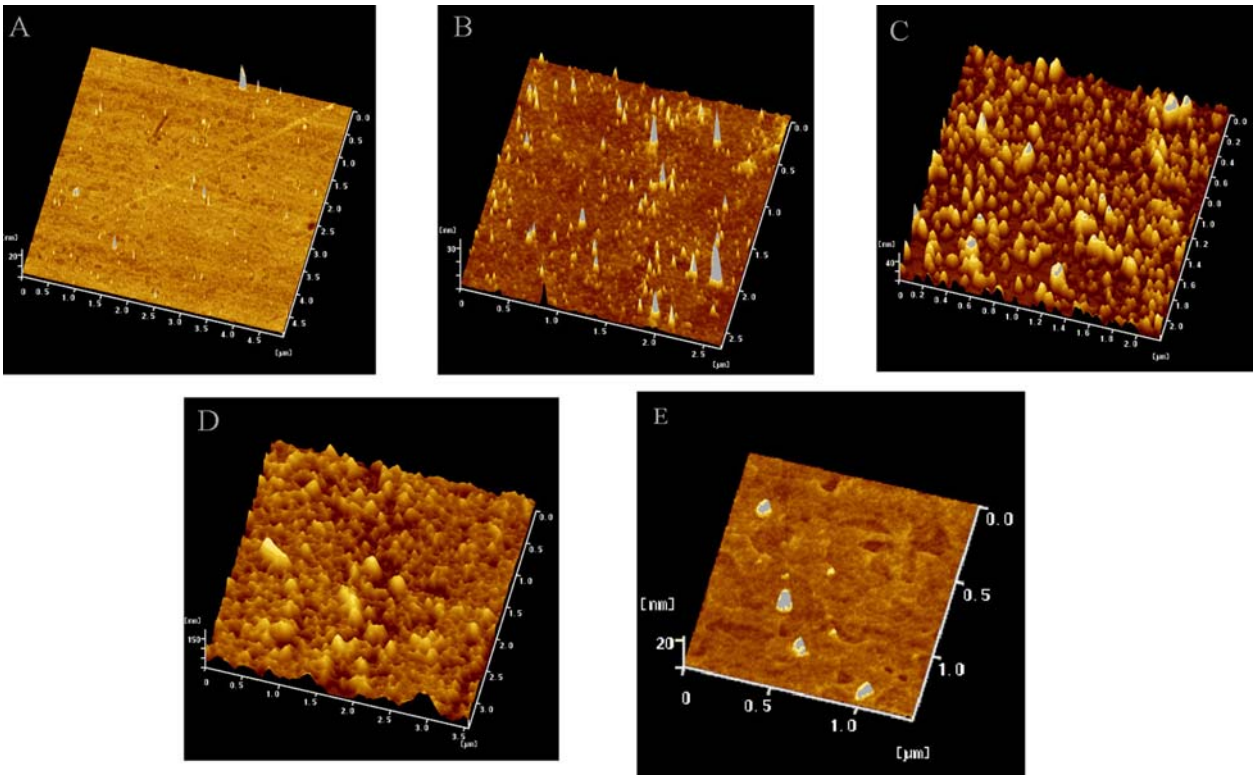

Figure 9. Tapping mode AFM images of the bare ITO electrode (A), CuMPCs modified electrode (B), the third layer CuHCF (C), the ninth layer CuHCF (D) and the ITO electrode obtained after cycled in $CuSO_4$ (E).

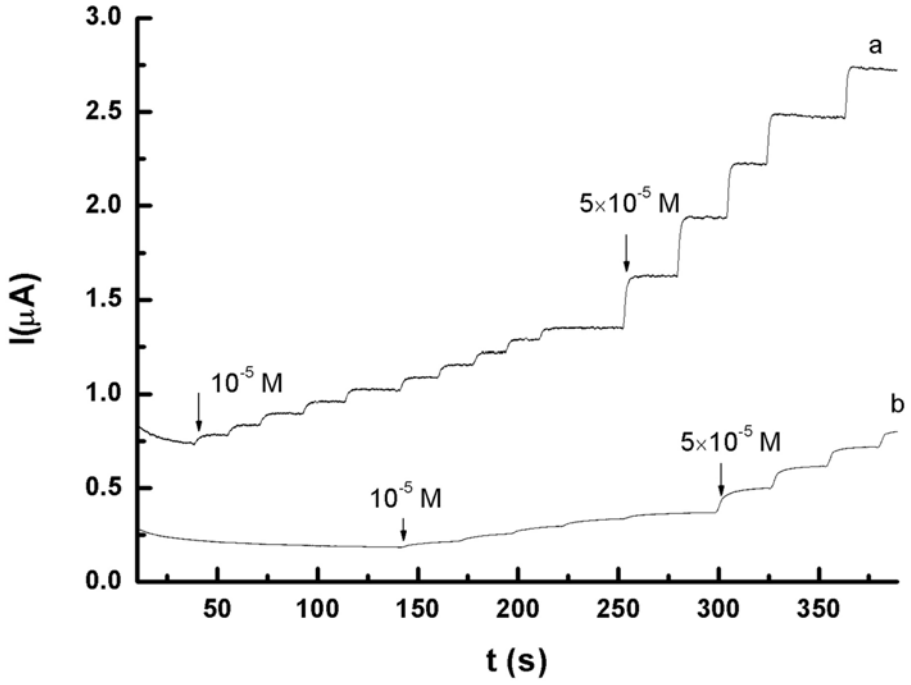

Figure 10. Typical steady-state response of the ninth layers CuHCF modified electrode (a) and the CuHCF layer prepared according to literature modified electrode (b) on successive injection of different concentration of H_2O_2 into 0.1 M stirring PBS 7.0 solution (containing 0.1 M KCl). Applied potential, 0 mV.

The energy required for crystal growth was smaller than that for the formation of new nuclei. When the surface was modified with the first layer of CuHCF, the activation energy related to the surface diffusion was increased. This in turn would decrease the surface diffusion length and promote the formation of the next CuHCF layer on the existing layer (50).

4.3. Application of multilayer CuHCF films as the H_2O_2 sensor

Prussian Blue and its analogous have been widely used as advanced transducers for hydrogen peroxide (51). Because of the high surface area of the 3-dimensional structure of the multilayes, the CuHCF film modified glassy carbon electrode showed high efficiency for the reduction of H_2O_2. Figure 10 a shows the typical responses of the ninthe layer CuHCF film modified electrode to the successive injections of hydrogen peroxide. A clearly defined reduction current proportional to the hydrogen peroxide concentration was observed. More than 100% enhancement over the CuHCF modified electrode can be observed (Figure 10 b), indicating the higher catalysis efficiency of the multilayer film. The responses occurred immediately after the addition of hydrogen peroxide and the time was less than 10 s to reach 95% of the steady-state value as shown in Figure 9. The response to hydrogen peroxide was linear in the concentration range of $5.0 \times 10^{-6} \sim 3.5 \times 10^{-4}$ M (RSD% = 0.9996). The detection limit was 1.0×10^{-6} M at a signal- to-noise ratio of 3.

4.4. Stability of the multilayer CuHCF films

The films formed by a galvanostatic or potentiostatic method from solutions of cupric ion and ferricyanide ion often showed the noticeable deterioration with the increase of the CV scans. However, the films obtained by the method were very stable. After cycling the electrode in a 0.1 M KCl solution for 1500 successive cycles between –0.20 and 0.90 V at a scan rate of 50 mV/s, negligible changes in the shape and height of the current of Fe(III)/Fe(II) were observed, which indicated that the formed films are very stable.

5. CONCLUSION

In conclusion, the cysteine monolayer protected copper clusters were used to bridge multilayer CuHCF films. The growth of the nanostructured film can be controlled by cycles of the electrochemical/chemical procedure. The obtained films have 3-dimensional (3-D) structure and could be used as the H_2O_2 sensor with higher efficiency. Since the approach can be applied to other systems, it will open the possibilities for the design of new 3-D molecular architectures.

6. ACKNOWLEDGMENTS

This work is supported by the National Natural Science Foundation of China (Grant No. 20635020, 20705030 and 20875081).

7. REFERENCES

1. Jonas Ekblom: Potential therapeutic value of drugs inhibiting semicarbazide-sensitive amine oxidase: vascular cytoprotection in diabetes mellitus. *Pharmacol Res*. 37, 87-92 (1998)

2. Ramón Rodrigo, Gonzalo Rivera: Renal damage mediated by oxidative stress: a hypothesis of protective effects of red wine. *Free Radical Biol. Med*. 33, 409-422 (2002)

3. Zhan Wang, Qiao Xu, Hai-Qiao Wang, Qin Yang, Jiu-Hong Yu, Yuan-Di Zhao:Hydrogen peroxide biosensor based on direct electron transfer of horseradish peroxidase with vapor deposited quantum dots. *Sensor Actuat B* 138, 278-282 (2009)

4. Yu Liu, Zhenyu Chu, Wanqin Jin: A sensitivity-controlled hydrogen peroxide sensor based on self-assembled Prussian Blue modified electrode, *Electrochem. Commun.* 11, 484-487 (2009)

5. Gabriela López de Lara Gonzáleza, Heike Kahlert, Fritz Scholza: Catalytic reduction of hydrogen peroxide at metal hexacyanoferrate composite electrodes and applications in enzymatic analysis, *Electrochim. Acta* 52, 1968-1974 (2007)

6. Ana P. Baioni, Marcio Vidotti, Pablo A. Fiorito, Susana I. Córdoba de Torresi: Copper hexacyanoferrate nanoparticles modified electrodes: A versatile tool for biosensors, *J. Electroanal. Chem.* 622, 219–224(2008)

7. Aissam Airoudj, Dominique Debarnot, Bruno Bche, Fabienne Poncin-Epaillard: Design and sensing properties of an integrated optical gas sensor based on a multilayer structure, *Anal. Chem*. 80, 9188–9194 (2008)

8. G. A. Somorjai: Introduction to surface chemistry and catalysis. *Wiley*: New York, 1994.

9. Chad A. Mirkin, Robert L. Letsinger, Robert C. Mucic, James J. Storhoff: A DNA-based method for rationally assembling nanoparticles into macroscopic materials. *Nature* 382, 607-609 (1996)

10. T. Andrew Taton, Robert C. Mucic, Chad A. Mirkin, Robert L. Letsinger: The DNA-mediated formation of supramolecular mono- and multilayered nanoparticle structures. *J. Am. Chem. Soc.* 122, 6305-6306 (2000)

11. Jwa-Min Nam, Savka I. Stoeva, Chad A. Mirkin: Bio-bar-code-based dna detection with pcr-like sensitivity. *J. Am. Chem. Soc.* 126, 5932-5933 (2004)

12. Nancy N. Kariuki, Li Han, Nam K. Ly, Melissa J. Patterson, Mathew M. Maye, Guojun Liu, Chuan-Jian Zhong: Preparation and characterization of gold nanoparticles dispersed in poly(2-hydroxyethyl methacrylate) *Langmuir* 18, 8255-8259 (2002)

13. Norifusa Satoh, Toshio Nakashima, Kimihisa Yamamoto. Metal-assembling dendrimers with a triarylamine core and their application to a dye-sensitized solar cell. *J. Am. Chem. Soc.* 127, 13030-13038 (2005)

14. Dirk M. Guldi, Israel Zilbermann, Greg Anderson, Nicholas A Kotov, Nikos Tagmatarchis, Maurizio Prato: Versatile organic (fullerene)−inorganic (CdTe nanoparticle) nanoensembles. *J. Am. Chem. Soc.* 126, 14340-14341 (2004)

15. Sudhanshu Srivastava, Benjamin L. Frankamp, Vincent M. Rotello: Controlled plasmon resonance of gold nanoparticles self-assembled with PAMAM dendrimers. *Chem. Mater.* 17, 487-490 (2005)

16. Erastus Gatebe, Hayley Herron, Rashid Zakeri, Pradeep Ramiah Rajasekaran, Samir Aouadi, Punit Kohli: Synthesis and characterization of polydiacetylene films and nanotubes. *Langmuir.* 24, 11947-11954 (2008)

17. Liqing Ma, David J. Mihalcik, Wenbin Lin: Highly porous and robust 4,8-connected metal−organic frameworks for hydrogen storage. *J. Am. Chem. Soc.* 131, 4610-4612 (2009)

18. Anat Hatzor, Tamar van der Boom-Moav, Shira Yochelis, Alexander Vaskevich, Abraham Shanzer, Israel Rubinstein: A metal-ion coordinated hybrid multilayer. *Langmuir* 16, 4420-4423 (2000)

19. Sarah E. Morgan, Paul Jones, Andrew S. Lamont, Andrew Heidenreich, Charles L. McCormick: Layer-by-layer assembly of pH-responsive, compositionally controlled (Co)polyelectrolytes synthesized via RAFT. *Langmuir* 23, 230–240 (2007)

20. Harry O. Finklea, Daniel A. Snider, John Fedyk, Eyal Sabatani, Yael Gafni, Israel Rubinstein: Characterization of octadecanethiol-coated gold electrodes as microarray electrodes by cyclic voltammetry and ac impedance spectroscopy. *Langmuir* 9, 3660-3667 (1993)

21. Michael J. Tarlov, John G. Newman: Static secondary ion mass spectrometry of self-assembled alkanethiol monolayers on gold. *Langmuir* 8, 1398-1405 (1992)

22. Chih-Ching Huang, Chao-Tsen Chen, Yen-Chun Shiang, Zong-Hong Lin, Huan-Tsung Chang: Synthesis of fluorescent carbohydrate-protected Au nanodots for detection of Concanavalin A and Escherichia coli. *Anal. Chem.* 81, 875-882 (2009)

23. Christopher J. Ackerson, Pablo D. Jadzinsky, Grant J. Jensen, Roger D. Kornberg: Rigid, specific, and discrete gold nanoparticle/antibody conjugates. *J. Am. Chem. Soc.* 128, 2635-2640 (2006)

24. Mathias Brust, Merryl Walker, Donald Bethell, David J. Schiffrin, Robin Whyman : Synthesis of thiol-derivatised gold nanoparticles in a two-phase Liquid–Liquid system. *J. Chem. Soc. Chem. Commun.* 801-802 (1994)

25. Marie-Christine Daniel, Didier Astruc: Gold nanoparticles: assembly, supramolecular chemistry, quantum-size-related properties, and applications toward biology, catalysis, and nanotechnology. *Chem. Rev.* 104, 293-346 (2004)

26. Partha S. Ghosh, Chae-Kyu Kim, Gang Han, Neil S. Forbes, Vincent M. Rotello: Efficient gene delivery vectors by tuning the surface charge density of amino acid-functionalized gold nanoparticles, *ACS Nano*. 2, 2213-2218 (2008)

27. Cristina Gentilini, Fabrizio Evangelista, Petra Rudolf, Paola Franchi, Marco Lucarini, Lucia Pasquato: Water-soluble gold nanoparticles protected by fluorinated amphiphilic thiolates, *J. Am. Chem. Soc.* 130, 15678-15682 (2008)

28. Jocelyn F. Hicks, Young Seok-Shon, Royce W. Murray: Layer-by-layer growth of polymer/nanoparticle films containing monolayer-protected gold clusters. *Langmuir* 18, 2288-2294 (2002)

29. E. Mateo Marti, Ch. Methivier, C. M. Pradier: (*S*)-Cysteine chemisorption on Cu(110), from the gas or liquid phase: an FT-RAIRS and XPS study. *Langmuir* 20, 10223-10230 (2004)

30. A. His, B. Lieberg: Chemisorption of L-cysteine and 3-mercaptopropionic acid on gold and copper surfaces: an infrared reflection-absorption study. *J. Colloid Interface Sci.* 144, 282-292 (1991)

31. Wen-Wei Zhang, Chang-Sheng Lu, Yang Zou, Jing-Li Xie, Xiao-Ming Ren, Hui-Zhen Zhu, Qing-Jin Meng: Self-assembly of L-cysteine-copper(II)/copper(I) multilayer thin films on gold, *J.Colloid Interf. Sci*. 249, 301-306 (2002)

32. M. M. Antonijevic and M. B. Petrovic: Copper corrosion inhibitors. A review. *Int. J. Electrochem. Sci.* 3, 1-28 (2008)

33. Saikat Mandal, Anand Gole, Neeta Lala, Rajesh Gonnade, Vivek Ganvir, Murali Sastry: Studies on the reversible aggregation of cysteine-capped colloidal silver particles interconnected via hydrogen bonds. *Langmuir* 17, 6262-6268 (2001)

34. S. Bharathi, M. Nogami, S. Ikeda: Layer by layer self-assembly of thin films of metal hexacyanoferrate multilayers. *Langmuir* 17, 7468-7471 (2001)

35. L. Pecci, G. Montefoschi, G. Musci, D. Cavallini: Novel findings on the copper catalysed oxidation of cysteine, *Amino Acids* 13, 355-367 (1997)

36. Joanne M. Elliott, Peter R. Birkin, Philip N. Bartlett, George S. Attard: Platinum microelectrodes with unique high surface areas. *Langmuir 15*, 7411-7415 (1999)

37. Lorraine M. Siperko1, Theodore Kuwana: Electrochemical and spectroscopic studies of metal hexacyanometalate films—III. Equilibrium and kinetics studies of cupric hexacyanoferrate. *Electrochim. Acta* 32, 765-771 (1987)

38. Mathias Brust, Peter M. Blass, Allen J. Bard: Self-assembly of photoluminescent copper(I)−dithiol multilayer

thin films and bulk materials. *Langmuir* 13, 5602-5607 (1997)

39. Celeste A. Constantine, Sarita V. Mello, Annie Dupont, Xihui Cao, David Santos, Jr., Osvaldo N. Oliveira, Jr., Francisco T. Strixino, Ernesto C. Pereira, Tu-Chen Cheng, Joseph J. Defrank, Roger M. Leblanc: Layer-by-layer self-assembled chitosan/poly(thiophene-3-acetic acid) and organophosphorus hydrolase multilayers. *J. Am. Chem. Soc*. 125, 1805-1809 (2003)

40. J. Ruths, F. Essler, G. Decher, H. Riegler: Polyelectrolytes I: polyanion/polycation multilayers at the air/monolayer/water interface as elements for quantitative polymer adsorption studies and preparation of hetero-superlattices on solid surfaces. *Langmuir* 16, 8871-8878 (2000)

41. Ph. Lavalle, C. Gergely, F. J. G. Cuisinier, G. Decher, P. Schaaf, J. C. Voegel, C. Picart: Comparison of the structure of polyelectrolyte multilayer films exhibiting a linear and an exponential growth regime: an in situ atomic force microscopy study**.** *Macromolecules* 35, 4458-4465 (2002)

42. C. Picart, J. Mutterer, L. Richert, Y. Luo, G. D. Prestwich, P. Schaaf, J. C. Voegel, P. Lavalle : Molecular basis for the explanation of the exponential growth of polyelectrolyte multilayers. *Proc. Natl. Acad. Sci*. 99, 12531-12535 (2002)

43. Lorraine M. Siperko, Theodore Kuwana: Electrochemical and spectroscopic studies of metal hexacyanometalate films. *J. Electrochem. Soc.* 396-402 (1983)

44. D. Ellis, M. Eckhoff , V. D. Neff: Electrochromism in the mixed-valence hexacyanides. 1. Voltammetric and spectral studies of the oxidation and reduction of thin films of Prussian blue. *J. Phys. Chem.* 85, 1225-1231 (1981)

45. Richard A. McAloney, Vyacheslav Dudnik, M. Cynthia Goh: Kinetics of salt-induced annealing of a polyelectrolyte multilayer film morphology. *Langmuir* 19, 3947-3952 (2003)

46. Dean M. DeLongchamp, Mark Kastantin, Paula T. Hammond: High-contrast electrochromism from layer-by-layer polymer films. *Chem. Mater.* 15, 1575-1586 (2003)

47. Mami Yamada, Masaya Arai, Masato Kurihara, Masatomi Sakamoto, Mikio Miyake: Synthesis and isolation of Cobalt hexacyanoferrate/chromate metal coordination nanopolymers stabilized by alkylamino ligand with metal elemental control. *J. Am. Chem. Soc.* 126, 9482-9483 (2004)

48. A. Lachenwitzer, S. Morin, O. M. Magnussen, R. J. Behm: In situ STM study of electrodeposition and anodic dissolution of Ni on Ag(111) *Phys. Chem. Chem. Phys.* 3, 3351-3363 (2001)

49. B. C. Bunker, P. C. Rieke, B. J. Tarasevich, A. A. Campbell, G. E. Fryxell, G. L. Graff, L. Song, J. Liu, J. W. Virden, G. L. McVay: Ceramic thin-film formation on functionalized interfaces through biomimetic processing. *Science* 264, 48-55 (1994)

50. P. P. Prosini, M.L. Addonizio and A. Antonaia: Effect of substrate surface treatment on the nucleation and crystal growth of electrodeposited copper and copper–indium alloys. *Thin Solid Films 298*, 191-196 (1997)

51. Arkady A. Karyakin: Prussian Blue and its analogues: electrochemistry and analytical applications. *Electroanalysis*, 13, 813-819 (2001)

Abbreviations: HCF: hexacyanoferrate; MHCF: metal hexacyanoferrate; CuHCF: copper hexacyanoferrate; MPC: monolayer-protected cluster; CuMPC: cysteine monolayer protected copper nanoparticle; SEM: scanning electron microscopy; AFM: atomic force microscopy

Key Words: CuMPCs, CuHCF, multilayer, H_2O_2, sensor

Send correspondence to: Jun-Jie Zhu, Key Lab of Analytical Chemistry for Life Science (MOE), Department of Chemistry, Nanjing University, Nanjing, 210093, China, Tel: 86-25-83594976, Fax: 86-25-83594976, E-mail: jjzhu@nju.edu.cn

http://www.bioscience.org/current/vol2E.htm